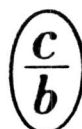


# **INSTRUMENTS AND EXPERIMENTAL TECHNIQUES**

**ПРИБОРЫ И ТЕХНИКА ЭКСПЕРИМЕНТА  
(PRIBORY I TEKHNIKA ÉKSPERIMENTA)**

**TRANSLATED FROM RUSSIAN**



**CONSULTANTS BUREAU, NEW YORK**

## MULTIPLIER ASSEMBLY OF THREE LARGE-FORMAT MICROCHANNEL PLATES FOR COORDINATE-SENSITIVE DETECTOR

F. I. Blatov, B. M. Glukhovskoi, M. A. Gruntman,  
A. A. Kozochkina, and V. B. Leonas

UDC 539.1.074

*An open-type multiplier assembly of three large-format plates for a coordinate-sensitive detector with high space resolution is described. The gain reaches  $8 \cdot 10^8$ , and the amplitude resolution is 0.2. The noise and load characteristics are given.*

Coordinate-sensitive detectors (CSD) based on microchannel plates (MCP) are designed for registration of ultraweak images created by discrete particle or photon fluxes. In systems with CSDs, the coordinates of the points of arrival at the sensitive surface of individual particles or photons are determined and recorded successively (in real time). The CSD is a most-promising type of detection device with a very wide range of realized and potential applications in scientific research [1-4].

A program for the creation of an MCP-based detection system for astrophysical applications was formulated and demonstrated earlier [5, 6]. The position of the point of incidence of a registered photon on the sensitive surface of the detector is determined by measurement of the coordinates of the "center of gravity" of the electron avalanche formed by means of charge division using a special collector. The actually attainable system characteristics include a sensitive-surface diameter of  $\geq 50$  mm, a space resolution of  $\geq 1000 \times 1000$  image elements, an accuracy of event referencing of  $\leq 1$  nsec, a multiplier-assembly noise of  $\leq 1 \text{ cm}^{-2}\text{sec}^{-1}$ , and a dead time (the processing time for one event) of  $\leq 1 \mu\text{sec}$ .

Such a detection system will obviously find wide use in experimental research in other areas.

The need to achieve the above characteristics imposes rigid requirements on the gain and amplitude resolution of the multiplier part of the system. In the present paper, which is an extension of our earlier work [5-8], we shall summarize the results of the first stage of the program and discuss the construction and list the characteristics of a open-type multiplier assembly of three MKP-56-15 large-format plates (with a diameter of 56 mm, a thickness of 0.8 mm, a channel diameter of 15  $\mu\text{m}$ , a distance between channel centers of 17  $\mu\text{m}$ , and an angle of  $8^\circ$  between the normal to the plate surface and the channel axis).

Several modifications of multiplier assemblies of three successive MCPs (so-called z-configuration) were developed and tested. A configuration of three plates is an optimum compromise between simplicity and convenience, on the one hand, and the multiplier-assembly characteristics that are to be achieved, on the other. A photograph of one of the modifications is provided in Fig. 1; the elements of the assembly have been described in detail [6]. The assembly consists of two main parts: a multiplier z-stage of three MCPs in a ceramic ring, which can be seen in Fig. 1; and a collector unit, which consists of six metal guard rings, a collector-anode, and a seating ring for the latter. Between the plates are the electrodes through which voltages are supplied to the plates and insulating spacers of photoglassceramic. The electrodes have a special shape that minimizes the number of obstructed MCP channels. These electrodes are produced by electroforming by building up on a matrix layers of metal of the required configuration (according to a template) and thickness (50  $\mu\text{m}$ ). The thicknesses of the insulating spacers are 0.8 and 0.4 mm; the sizes of the first and second spaces between the plates (counting from the input side) are 0.9 and 0.5, respectively. The guard rings receive voltages that ensure a uniform potential drop in the drift space between the output of the multiplier and the collector. A uniform electrostatic field allows the radial position (coordinates) of the "center of gravity" of an electron avalanche to be preserved as it is transported to the collector.

---

Institute of Mechanics Problems, Academy of Sciences of the USSR, Moscow. Translated from *Pribory i Tekhnika Éksperimenta*, No. 3, pp. 152-155, May-June, 1990. Original article submitted May 17, 1989; revision submitted August 16, 1989.

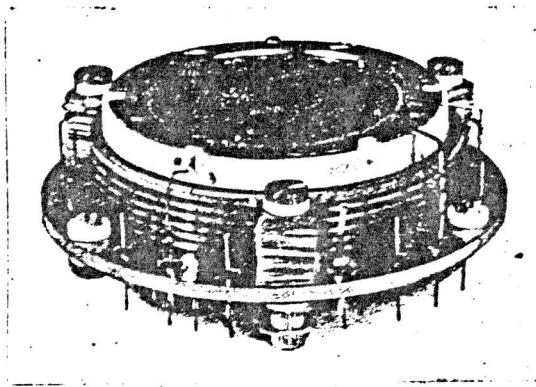


Fig. 1. Multiplier assembly of three large-format micro-channel plates.

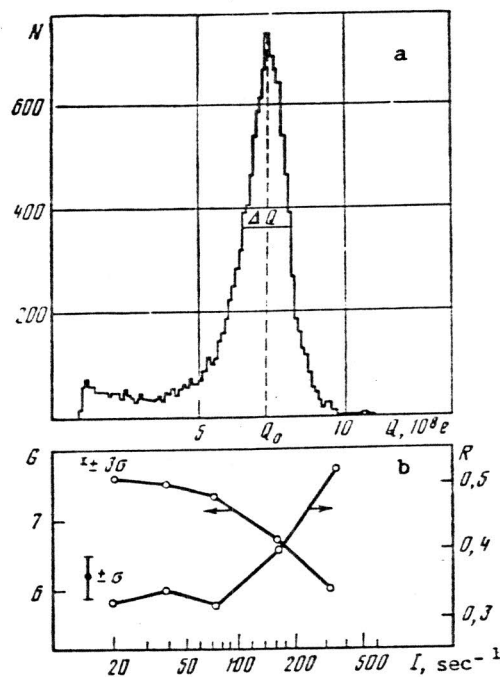


Fig. 2. a) Pulse-amplitude distribution:  $\Delta Q$ ) full width at half maximum;  $Q_0$ ) gain;  $R = \Delta Q/Q_0 \approx 0.2$ . b) Gain  $G$  and amplitude resolution  $R$  as functions of load  $I$ .

The use of a wedge-and-strip collector assembly [4, 9-11] is most-promising for obtaining a high space resolution. The diameter of the working surface area of the installed detector is 63 mm. The collector elements (strips, wedges, and coil) are deposited by standard microelectronic technology with subsequent etching of a photographic image of the collector and leads. Silicon wafers (76 mm in diameter and 0.38 mm thick) that are usually employed in integrated-circuit fabrication are used as collector-anode substrates. A thorough description of the design and fabrication technology of the collector-anode will be provided in a separate publication. Since coordinate measurements were beyond the scope of the present work, the collector leads were connected together to study the characteristics of the assembly.

The assembly (Fig. 1) was tested with prolonged heating in vacuum at temperatures of up to 300°C and can therefore serve as the basis for the creation of a sealed photodetector (PCSD).

When studied in the single-particle-count mode, the multiplier assembly was irradiated in a vacuum of  $2 \cdot 10^{-6}$  torr by a beam of Ar atoms with an energy of 3 keV; it was also possible to irradiate the assembly with ultraviolet photons. As has been shown [5, 7], similar results are obtained in both cases. The gain and amplitude resolution were studied as functions of the

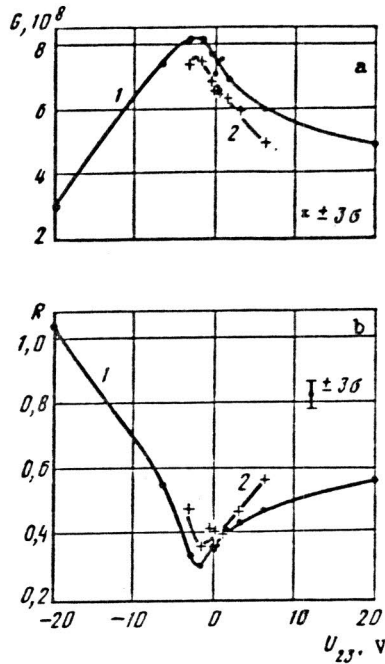


Fig. 3. Gain  $G$  and amplitude resolution  $R$  as functions of voltage  $U_{23}$  in gap between second and third MCPs. Voltages  $U_1:U_{12}:U_2:U_3:U_{3c} = 880:30:1100:1100:140$  V and  $860:30:1000:1000:140$  V for curves 1 and 2, respectively ( $U_i$  is the voltage on the  $i$ -th plate, and  $U_{ij}$  is the voltage between the  $i$ -th plate and  $j$ -th plate or collector (c)).

voltages on and between the plates and also of the load. The gain  $G$  is understood as the most-likely pulse amplitude, which is expressed by the total electron charge of the output avalanche (the quantity  $Q_0$  in the typical amplitude distribution shown in Fig. 2a). The amplitude resolution  $R = \Delta Q/Q_0$  is the ratio of the full width ( $\Delta Q$  in Fig. 2a) at half maximum of the amplitude distribution to the most-likely pulse amplitude. The measurement procedure has been discussed earlier [5-8] and will not be examined in detail here.

Two types of detector illumination are possible: distributed over the sensitive surface and point. In our case, the diameter of the irradiating beam was 0.6 mm, and the size of the electron avalanche at the entrance to the third MCP was 1.5-2 mm, which allows point illumination to be assumed [6].

The principal measurements were made with a detector count rate  $I \approx 40 \text{ sec}^{-1}$ . Typical load curves are shown in Fig. 2b. The load  $I \approx 40 \text{ sec}^{-1}$ , the exceeding of which causes  $G$  to decrease and  $R$  to rise, is considerably below the critical value  $I_{cr}$ . The deterioration of performance with an increase in load is continuous (Fig. 2b); therefore, the choice of an  $I_{cr}$  value is somewhat arbitrary. The load at which the maximum of the distribution was shifted in the lower-amplitude direction by  $1/2 \Delta Q_0$  ( $\Delta Q_0$  corresponds to extremely small loads [6]) was taken for  $I_{cr}$ . For the described array,  $I_{cr} \approx 300 \text{ sec}^{-1}$ , which allows the recovery time of an MCP channel to be estimated as  $\tau \approx 3 \text{ msec}$ . It is apparent from Fig. 2b that the gain remains high — only 20% below  $G_0$  — at this  $I_{cr}$  value. The amplitude resolution is more sensitive to the load — it reduced to  $R \approx 0.5$  — but the distribution remains saturated. The array can obviously be used successfully when  $I > I_{cr}$ ; the actual load limit in each case must be determined by the specific nature of the task.

The high gain and narrow pulse-amplitude distribution allow a high space resolution to be achieved in coordinate measurements. The  $G \approx 8 \cdot 10^8$  that we obtained is a record-high value; it is important that  $R \approx 0.2$  could be obtained simultaneously (Fig. 2a). These characteristics were obtained by optimization of the distribution of the voltages on and between the plates. As was to be expected, with an increase in the voltage on each of the plates, the gain rose and the amplitude distribution was gradually narrowed.

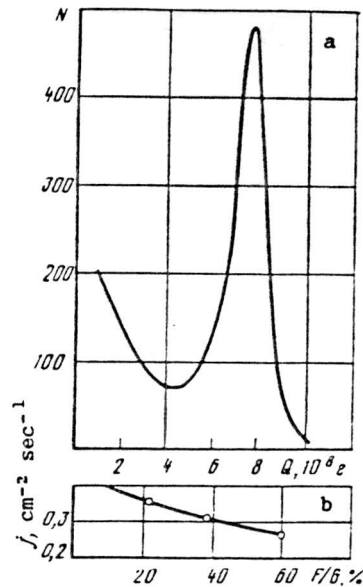


Fig. 4. Noise characteristics of assembly: a) amplitude distribution of noise pulses; b) count rate  $j$  of noise pulses as a function of discrimination threshold  $F$  ( $N$  is the number of counts,  $Q$  is the charge of the electron avalanche, and the gain  $G = 7.7 \cdot 10^8$ ).

The voltage on the first MCP  $U_1 \leq 900$  V was limited by the increase in the noise-count rate. The voltages between the plates affect the characteristics of the assembly differently: the voltage  $U_{12}$  between the first and second plates weakly and the voltage  $U_{23}$  between the second and third plates strongly. A graph of  $G(U_{23})$  is provided in Fig. 3a. It can be seen that the gain has an extreme; a variation of  $U_{23}$  by only 5 V reduces  $G$  by 15%. The nature of the dependence is qualitatively clear: the accelerating voltage impedes the dispersion of the avalanche electrons and focuses them, thereby reducing the number of "irradiated" channels of the third MCP. The cutoff voltage has a similar effect in reducing the number of "irradiated" channels — the electrons whose longitudinal energy is less than  $eU_{23}$  are intercepted. The amplitude distribution is also strongly dependent on  $U_{23}$  (Fig. 3b).

The maximum gain  $G = 8 \cdot 10^8$  for  $R = 0.2$  was obtained with the following voltages on the assembly:  $U_1 = 880$  V,  $U_{12} = 30$  V,  $U_2 = 1100$  V,  $U_{23} = -2$  V,  $U_3 = 1100$  V, and  $U_{3c} = 140$  V. This voltage distribution is optimal for the described multiplier assembly. However, the study of different assemblies has shown good reproducibility of the characteristics: the spread of  $G$  values is within a factor of 2 and the spread of  $R$  is  $\pm 30\%$ .

An important characteristic that determines the dynamic range of a CSD (image contrast) is the internal noise of the multiplier system. The noise-count rate is very sensitive to the design features of the assembly and the operating conditions. Assembly noise is conveniently characterized by the amplitude distribution of the noise pulses and by the noise-count rate for various discrimination thresholds, which are expressed in fractions of  $G$ . A typical noise-pulse amplitude distribution and a graph of the noise-count rate as a function of the discrimination threshold are provided in Fig. 4. It is apparent that the distribution has a clearly expressed peak in the amplitude region corresponding to the nominal gain, which was not observed by Siegmund et al. [12], for example. This is evidently due to differences in the MCP fabrication technology. The noise-count rate is  $0.4 \text{ cm}^{-2} \text{sec}^{-1}$  for a discrimination threshold of  $0.1G$  and is practically equal to the corresponding value of Siegmund et al. [12].

The described multiplier assembly of three large-format MCPs has a gain of up to  $8 \cdot 10^8$ , a resolution of 0.2, and an internal-noise level of  $0.4 \text{ cm}^{-2} \text{sec}^{-1}$ . These characteristics are already providing vast opportunities for numerous applications. The characteristics that have been achieved and the results of thermal and mechanical tests of the array allow it be used as the basis for an evacuated PCSD.

#### LITERATURE CITED

1. M. Lampton, Proc. Intern. Astron. Union Colloq. 40, Meudon Observ., France (1977), p. 32.

2. R. W. van Resandt Wijnaendts and J. Los, Proc. Intern. Conf. Phys. El. Atom. Coll., North Holland, Netherlands (1980), p. 831.
3. J. G. Timothy, Publ. Astron. Soc. Pac. 1983, **95**, No. 573, 831 (1983).
4. M. A. Gruntman, Prib. Tekh. Éksp., No. 1, 14 (1984).
5. M. A. Gruntman and A. A. Demchenkova, Prib. Tekh. Éksp., No. 5, 146 (1986).
6. M. A. Gruntman, A. A. Kozochkina, and V. B. Leonas, Preprint Inst. Space Res. No. 1270, Moscow (1987).
7. M. A. Gruntman and A. A. Demchenkova, Preprint Inst. Space Res. No. 1001, Moscow (1985).
8. A. A. Demchenkova, Prib. Tekh. Éksp., No. 5, 149 (1987).
9. C. Martin, P. Jelinsky, M. Lampton, et al., Rev. Scient. Instrum., **52**, No. 7, 1067 (1981).
10. M. A. Gruntman, Candidate's Dissertation, Inst. Space Res., Moscow (1983).
11. M. A. Gruntman and V. B. Leonas, Prib. Tekh. Éksp., No. 1, 257 (1985).
12. O. H. W. Siegmund, M. Lampton, J. Bixler, et al., J. Opt. Soc. Am. A, **3**, 2139 (1986).

## SINGLE-ELECTRON CHARACTERISTICS OF FÉU-147 PHOTOMULTIPLIERS

B. M. Glukhovskoi and I. F. Yaroshenko

UDC 621.383.292

*The single-electron characteristics of FÉU-147 compact high-speed photomultipliers are measured. Measurement of the individual components of the output-pulse amplitude distribution showed that the exponential branch was due to noise pulses and afterpulses. It is concluded that selected FÉU-147 specimens could be used in threshold measurements.*

The use of high-speed photomultipliers (PM) in photon-counting devices allows the dynamic range of the received signals to be expanded and the measurement accuracy to be increased. The compact FÉU-147, which has fairly good time parameters in the photon-counting mode, is of interest in this connection. The single-electron characteristics of a PM provide the most complete representation of its threshold properties in the photon-counting mode. In particular, measurement of the single-electron-pulse amplitude distribution (SEPAD) at the PM output and investigation of the causes of its individual components allow an optimum discrimination threshold to be selected and criteria for device selection for threshold measurement to be obtained [2].

The radiation source in the measurements was a timing light-emitting diode, which produced light pulses with a duration of 6 nsec and a repetition frequency of 100 kHz. A light spot 1 mm in diameter was focused on the center of the photocathode. The radiation flux from the light-emitting diode was attenuated by neutral light filters to a level at which single-electron pulses caused by individual photoelectrons were formed at the PM output. The PM output pulses were amplified by an amplifier with a bandwidth of 100 MHz and fed to either an integrating or a differential discriminator. The maximum attainable pulse repetition frequency was 120 MHz for the wideband amplifier and discriminator. The 50-mV window of the differential discriminator was shifted from 0.06 to 2.2 V at a rate of 0.033 V/sec. To isolate single-photoelectron pulses and afterpulses, the discriminator output was connected to a coincidence circuit, which also received strobe pulses with durations of 0.05 and 0.5  $\mu$ sec [3]. The SFPAD was observed on the screen of an S8-14 storage oscilloscope. The voltage divider recommended by the PM producer was used.